archives
of thermodynamics
Vol. **41**(2020), No. 4, 147–168
DOI: 10.24425/ather.2020.135857

Quantity and quality of marine dual-fuel engine's exhaust sensible waste heat considering different sulfur content in fuels

MATEUSZ PRZYBYŁA*
ANDRZEJ ADAMKIEWICZ

Maritime University in Szczecin, Wały Chrobrego 1-2, 70-500, Szczecin, Poland

Abstract Maritime transport is facing a set of technical challenges due to implementation of ecological criterions on 1st Jan. 2020 and 2021 by the International Maritime Organization. The advantageous properties of natural gas (NG) as fuel in conjunction with dual-fuel (DF) internal combustion engines (ICE) potentially enables the fulfilment of all criterions. Moreover the 2020 global sulfur cap in combination with its low content in NG potentially enables to recover higher rates of waste heat and exergy of exhaust gas without the risk of low temperature corrosion. In this study the influence of sulfur content in NG and pilot fuel oil (PFO) on the sulfuric acid condensation temperature was investigated in order to determine the rate of waste heat (quantity) and exergy (quality) of four-stroke DF IC engine's exhaust for 50%, 85% and 100% of engine load. Determined parameters were compared with two sets of reference values calculated for the same engine: a) fueled with NG and PFO with fixed minimum exhaust temperature set as 423.15 K, b) fueled with 3.5% sulfur mass fraction fuel oil only with variable minimum exhaust gas temperature. The results show that the assumption of case a) can lead to significant reduction of recovered rates of exhaust waste heat and exergy in the ranges of 10% to 24% and 43% to 57%, respectively. Higher values were obtained for case b) where the ranges of unrecovered rate of heat and exergy achieved 20% to 38% and 60% to 70%.

Keywords: Waste heat recovery system; Dual-fuel internal combustion engine; Natural gas; Sulfuric acid condensation

*Corresponding Author. Email: mateusz.przybyla@wp.pl

Nomenclature

B – exergy, J
$\dot{B}$ – exergy transfer rate, W
$\tilde{b}$ – molar specific flow exergy, J/mol
$\tilde{c}_p$ – molar isobaric specific heat, J/molK
$\tilde{h}$ – molar specific enthalpy, J/mol
M – molecular weight, g/mol
n – rotational speed 1/min
$\dot{n}$ – molar flow rate, mol/s
p – pressure, Pa
$\dot{Q}$ – heat transfer rate, W
$\tilde{s}$ – molar specific entropy, J/molK
T – thermodynamic temperature, K
V – volume, m^3
W – work, J
$\dot{W}$ – work transfer rate – power, W
x – mass fraction, kg/kg
Y – mole ratio, mol/mol
y – mole fraction, mol/mol

Greek symbols

α – number of carbon atoms
β – number of hydrogen atoms
Γ – engine load
γ – number of oxygen atoms
δ – number of sulfur atoms
ε – molar oxygen-fuel/air-fuel ratio
λ – excess air coefficient
φ – ambient air relative humidity
ψ – waste heat quality index

Subscripts and superscripts

0 – ambient conditions
1 – exhaust gas state at turbocharger outlet
2 – exhaust gas state at the end of waste heat conversion process
a – air
c – condensation
d – dry composition
e – effective
ex – exhaust gas
f – fuel
i – components of natural gas
j – components of fuel oil/pilot fuel oil
k – components of combustion products
R – parameter reference value determined for liquid fuel oil mode of analyzed engine

r	–	parameter reference value determined for fixed minimum exhaust gas temperature
s	–	stoichiometric
sat	–	saturation state
$(\sim)$	–	molar quantity

Acronyms

CI	–	compression-ignition
CPP	–	controllable pitch propeller
DF	–	dual-fuel
ECA	–	emission control area
FO	–	fuel oil
GT	–	gas turbine
HFO	–	heavy fuel oil
IC	–	internal combustion
ICE	–	internal combustion engine
IMO	–	International Maritime Organization
LNG	–	liquefied natural gas
LNGC	–	liquefied natural gas carrier
LNGFS	–	liquefied natural gas fueled ship
MDO	–	marine diesel oil
NG	–	natural gas
PFO	–	pilot fuel oil
ST	–	steam turbine
SCR	–	selective catalytic reduction
SRC	–	steam Rankine cycle
WHRS	–	waste heat recovery system
2S-DF-HP	–	two-stroke DF CI engine with high-pressure gas injection
2S-DF-LP	–	two-stroke DF CI engine with low-pressure gas injection
2S-FO-CI	–	two-stroke CI engine
4S-DF-CI	–	four-stroke DF CI engine
4S-NG-SI	–	four-stroke NG fueled spark-ignition engine

1 Introduction

The decision made by the International Maritime Organization (IMO) on the simultaneous implementation of regulations on 01 January 2020 regarding the global sulfur content in marine fuel and the energy efficiency of ships poses a new, complex set of problems for maritime transport. In the case of vessels operated within the Baltic and North Sea areas this set of problems is extended by the implications resulting from the decision to classify them on 1 Jan. 2021 as Emission Control Area (ECA) [1].

Using low-sulfur fuel (fuel with sulfur mass fraction not exceeding 0.5% or 0.1%) eliminates the necessity of using sulfur oxides emission reduction

methods (e.g. scrubbers) in order to meet the first of abovementioned IMO criterion, but leaves the problem of excessive emission of nitrogen oxides unsolved. Meeting the Tier III criterion implies the need to process combustion products in the selective catalytic reduction (SCR) system [2]. On the other hand, the SCR system significantly limits the possibility of exhaust waste heat conversion due to the required minimum temperature determining the efficiency of the process [2]. In addition, the amount of available waste heat flux of liquid fuel combustion products and the efficiency of its conversion is limited mainly by the condensation temperature of the sulfuric acid [3].

Liquefied natural gas (LNG) is an alternative marine fuel that reduces the problems described above. The advantages arising from fueling of marine dual-fuel (DF) internal combustion engines (ICE) by natural gas (NG) in comparison with marine fuel oils, e.g.: lower specific emission of SO_x, NO_x, CO_2, higher fuel conversion efficiency, the degree of freedom in choosing marine fuel type for ship propulsion acc. to its actual price (taking into consideration IMO regulations), led to: a) significant change from 72% of quantitative shares of the liquefied natural gas carriers (LNGC) power systems with steam turbines (ST) in 2015 to 50%–50% shares with ICE at the end of 2018 (Fig. 1) [4], b) formation of liquefied natural gas fueled ships (LNGFS) population (Fig. 1).

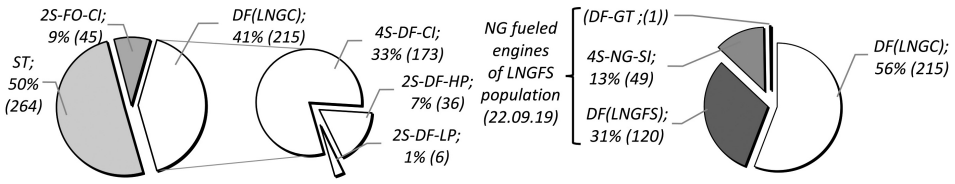

Figure 1: Quantitative shares of: a) heat engines in LNGC population and b) NG fueled IC marine engines in LNGC and LNGFS population (DF gas turbine not included), where: ST – steam turbines, 2S-FO-CI – two-stroke compression-ignition (CI) engines, 4S-DF-CI – four-stroke DF CI engines, 2S-DF-HP – two-stroke DF CI engines with high-pressure gas injection, 2S-DF-LP – two-stroke DF CI engines with low-pressure gas injection, DF-GT – DF gas turbine, 4S-NG-SI – four-stroke NG fueled spark-ignition engines [4, 5].

The lower specific emission of SO_x, NO_x and CO_2 and higher fuel conversion efficiency enables the fulfilment of the IMO ecological criteria. More-

over, following observations are pointing out the possibilities of increasing the rate of recovered waste heat of DF ICE exhaust:

- possibility of significant reduction of the minimum exhaust gas temperature due to the insignificant sulfur content in LNG [6–9];
- higher temperatures of NG combustion products in the turbocharger outlet in comparison with FO [2];
- the possibility of utilizing waste heat at low temperatures in cycles with an organic working medium [10–15];
- evolution of marine organic Rankine cycle (ORC) waste heat recovery systems (WHRS), which is proved by the physical implementation of such a system described in [16].

A different position regarding first of abovementioned observation is presented in [17, 18] warning about the observed sulfur content in natural gas that may lead to condensation of sulfuric acid on the heat transfer surface. Basing on this contradiction the analysis of studies treating about exhaust waste heat recovery from marine IC engines has been made. The selected studies with analyzed parameters, i.e. exhaust minimum temperature and sulfur mass fraction in fuel, are shown in Table 1.

Table 1: Selected studies of waste heat recovery from exhaust gas of marine internal combustion engines.

Theoretical cycle	ICE type	Fuel	x_S	$T_{ex(\min)}$, K	Reference
[a] SRC/ORC	2S-FO-CI	[d] HFO	0.030	421.15	[7]
SRC/ORC	2S-FO-CI	[e] MDO	0.005	398.15	[7]
SRC	4S-DF-CI	HFO	–	433.15	[8]
SRC	4S-DF-CI	NG/HFO	–	Unlimited	[8]
ORC	4S-DF-CI	NG/FO	–	323.15	[11]
ORC	4S-FO-CI	FO	0.001	$358.15 \leq T_{ex(\min)} \leq 363.15$	[12]
ORC	4S-DF-CI	NG/FO	–	$353.15 \leq T_{ex(\min)} \leq 373.15$	[13]
[b] ORC	4S-DF-CI	NG/FO	–	$363.15 \leq T_{ex(\min)} \leq 423.15$	[14]
[c] ORC	4S-DF-CI	NG/FO	–	373.15	[15]

[a] SRC – steam Rankine cycle, [b] boil off gas as a cold sink, [c]LNG as a cold sink, [d] HFO – heavy fuel oil, [e] MDO – marine diesel oil.

Most of the studies assumes fixed minimum exhaust gas temperature and does not relate this parameter with sulfur mass fraction by mathematical function. These assumptions can potentially lead to the limitation of the recovered rate of waste heat and exergy. In the case of the dual-fuel ICE population (Fig. 1), which is the most numerous, the sulfur present in the combustion process is fed in natural gas and also in pilot fuel oil (PFO) in the amount resulting from the IMO regulation. That is why this study considers the influence of sulfur content in NG and pilot fuel oil on:

a) sulfuric acid condensation temperature,

b) amount of available exhaust gas waste heat (quantity),

c) exergy of exhaust gas (quality),

d) thermodynamic system efficiency gain assuming ideal waste heat conversion process (exergy based),

e) ratio of heat and exergy and their maximum values when equilibrium with surroundings is reached.

The thermodynamic analysis has been made for 50%, 85% and 100% load of four-stroke DF ICE when fueled with NG and PFO with different sulfur content. The same parameters have been determined for two reference cases. First assumes fixed minimum exhaust gas temperature $T_{ex(\min)} = 423.15$ K and the same fuelling modes. The second assumes variable minimum exhaust gas temperature and fueling only with fuel oil with 3.5% mass fraction of sulfur. All of the sets of determined parameters have been compared with each other.

2 Thermodynamic analysis

The examined research problem is of *a posteriori* type and considers physically existing marine dual-fuel four-stroke compression ignition (4S-DF-CI) engine MAN 9L51/60DF dedicated for propulsion of controllable pitch propeller (CPP). In this type of problem the geometrical parameters of engine, i.e. total swept volume $V = 1,1025$ m^3 and the operational parameters of working cycle, e.g. crankshaft rotational speed $n = 500$ 1/min, maximum effective power $\dot{W} = \sum_{c=1}^{9} \dot{W}_c = 9450$ kW (where $c = \{1, 2, \ldots, 9\}$ represents

the assumed number of cylinders), are determined and are not subject of modification.

As the subject of this study the exhaust gas of chosen engine were considered. Thermodynamic analysis was carried for an open steady-state thermodynamic system presented in Fig. 2, assuming surroundings parameters $p_0 = 101.325$ kPa, $T_0 = 298.15$ K, and $\varphi_0 = 0.3$.

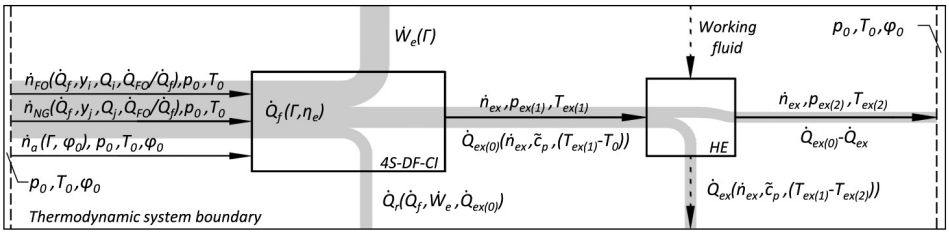

Figure 2: Diagram of studied thermodynamic system with simplified analyzed parameters relations.

Some of the substance balance parameters has been calculated based on the energy balance of selected engine working cycle using the first two of the graphs presented in Fig. 3, i.e., effective efficiency and the fuel energy ratio of PFO. The rest of the ICE parameters which are dry air molar flow rate and exhaust gas temperature at the turbocharger outlet were assumed as presented in Fig. 3.

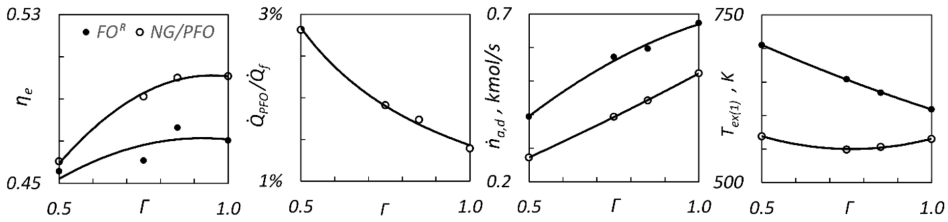

Figure 3: Selected parameters of MAN 9L51/60DF: effective efficiencies, the PFO energy shares, molar flow rates of dry air and exhaust gas temperature at the outlet of turbocharger, as a function engine load [2].

The assumed fuels composition and lower heating values of components (Table 2) has been used in the substance balance to determine the amount of fuels and the combustion products composition.

Using the composition of combustion products, the condensation temperature of sulfuric acid and isobaric specific heat as a function of temperature were determined. The specific heat has been related with the

Table 2: Composition and basic properties of natural gas and marine fuel oil used in this study.

$i,\ j^a$	Fuel	α_i, α_j	β_i, β_j	γ_i, γ_j	δ_i, δ_j	$y_i, y_j(x_j)$	$x_i(y_i), x_j$	$\widetilde{Q}_i, \widetilde{Q}_j$ kJ/mol
$i=1$	CH_4	1	4	0	0	$1-\sum_{i=2}^{6} y_i$	$\frac{y_i M_i}{\sum_{i=1}^{6} y_i M_i}$	802.77
$i=2$	C_2H_6	2	6	0	0	0.084		1431.66
$i=3$	C_3H_8	3	8	0	0	0.030		2043.15
$i=4$	C_4H_{10}	4	10	0	0	0.012		2657.54
$i=5$	C_5H_{12}	5	12	0	0	0.002		3271.50
$i=6$	S_i	0	0	0	1	$\{1\times10^{-6}, \cdots, 2\times10^{-5}\}$		296.83
$j=1$	$C_{12}H_{26}$	12	26	0	0	$\frac{x_j}{M_j \sum_{j=1}^{2} \frac{x_j}{M_j}}$	$1-x_S$	7592.29
$j=2$	S_j	0	0	0	1		$\{0.001, \cdots, 0.035\}$	296.83

[a] Species have been denoted with subscripts $i = \{1, 2, \ldots, 6\}$ for NG and $j = \{1, 2\}$ for PFO.

temperature using polynomial function later used to establish the rates of waste heat and thermal exergy. Using calculated values, the following was assessed: quality of the waste heat source using the waste energy quality index, the ratio of the calculated rates of waste heat and thermal exergy to their maximum values (i.e. when thermal equilibrium with surroundings is reached), comparison of abovementioned parameters with two sets of reference parameters. More detailed assumptions are made parallel with thermodynamic formulas presentation and description.

2.1 Energy and substance balances of dual-fuel internal combustion engine steady-state working process

The presented balance of energy transferred through the thermodynamic system boundary (Fig. 2) in the form of heat and work was based on energy conservation principle

$$\dot{Q}_f = \dot{Q}_{\mathrm{NG}} + \dot{Q}_{\mathrm{PFO}} = \dot{W}_e + \dot{Q}_{ex(0)} + \dot{Q} = f(\Gamma), \tag{1}$$

where the rate of fuels energy as a function of effective power and efficiency was calculated using assumed parameters (Fig. 3)

$$\dot{Q}_f = \dot{Q}_{\mathrm{NG}} + \dot{Q}_{\mathrm{PFO}} = \frac{\dot{W}_e}{\eta_e} = \frac{\dot{W}_e}{\dot{W}_e/\dot{Q}_f}\,, \tag{2}$$

$$\dot{Q}_{\mathrm{PFO}} = \dot{Q}_f \frac{\dot{Q}_{\mathrm{PFO}}}{\dot{Q}_f} = \frac{\dot{W}_e}{\eta_e} \frac{\dot{Q}_{\mathrm{PFO}}}{\dot{Q}_f}, \quad \dot{Q}_{\mathrm{NG}} = \dot{Q}_f - \dot{Q}_{\mathrm{PFO}} = \frac{\dot{W}_e}{\eta_e} - \dot{Q}_{\mathrm{PFO}}. \tag{3}$$

To determine the maximum rate of exhaust gas waste heat using following equation:

$$\dot{Q}_{ex(0)} = \dot{n}_{ex} \left[\tilde{h}_{ex}(T_{ex(1)}) - \tilde{h}_{ex}(T_0) \right] = \dot{n}_{ex} \Delta \tilde{h}_{ex(0)}, \tag{4}$$

firstly, the presented balance of incoming and outgoing molar flow rates crossing the thermodynamic system boundary (Fig. 2) based on matter conservation principle have to be solved

$$\dot{n}_f + \dot{n}_a = \dot{n}_{\mathrm{NG}} + \dot{n}_{\mathrm{PFO}} + \dot{n}_a = \sum_{i=1}^{6} \dot{n}_i + \sum_{j=1}^{2} \dot{n}_j + \dot{n}_a = \sum_{k=1}^{n} \dot{n}_k = \dot{n}_{ex}, \tag{5}$$

The rate of rejected heat $\dot{Q}$ was determined as a last unknown variable of energy balance (1).

Molar flow rates and fractions of both fuels entering the control volume were determined on the basis of Eqs. (3) and (6) and assumed fuels compositions and lower heating values of their components (Table 1)

$$\begin{aligned} \dot{n}_{\mathrm{NG}} &= \frac{\dot{Q}_{\mathrm{NG}}}{\sum_{i=1}^{6} y_i \widetilde{Q}_i}, \qquad & y_{\mathrm{NG}} &= \frac{\dot{n}_{\mathrm{NG}}}{\dot{n}_f}, \\ \dot{n}_{\mathrm{PFO}} &= \frac{\dot{Q}_{\mathrm{PFO}}}{\sum_{j=1}^{2} y_j \widetilde{Q}_j}, \qquad & y_{\mathrm{PFO}} &= \frac{\dot{n}_{\mathrm{PFO}}}{\dot{n}_f}. \end{aligned} \tag{6}$$

The molar flow rate of air was calculated as the sum of assumed molar flow rate of dry air (Fig. 3) and molar flow rate of water vapor

$$\dot{n}_a = \dot{n}_{a,d} + \dot{n}_{\mathrm{H_2O}(a)} = \dot{n}_{a,d} \left(1 + Y_{\mathrm{H_2O}}\right), \tag{7}$$

where the mole ratio of water vapor contained in the dry air related with assumed surroundings parameters was calculated using relation

$$Y_{\mathrm{H_2O}} = \frac{n_{\mathrm{H_2O}}}{n_{a,d}} \equiv \frac{p_{\mathrm{H_2O}}}{p_0 - p_{\mathrm{H_2O}}} = \frac{\varphi_0 p_{\mathrm{H_2O}(sat)}}{p_0 - \varphi_0 p_{\mathrm{H_2O}(sat)}}, \tag{8}$$

and Antoine equation with the coefficients according to [19]

$$p_{\mathrm{H_2O}(sat)} = \exp\left(A - \frac{B}{T + C}\right) = \exp\left(16.262 - \frac{3799.89}{T - 46.38}\right). \tag{9}$$

2.2 Stoichiometric combustion balance of quasi-molecule $C_\alpha H_\beta O_\gamma S_\delta$

Due to a significant number of NG and PFO constituents the analysis of the combustion process was based on the presented stoichiometric combustion balance of quasi-molecule $C_\alpha H_\beta O_\gamma S_\delta$ of fuel

$$C_\alpha H_\beta O_\gamma S_\delta + \lambda\varepsilon_s\,(O_2 + 3.76N_2) \longrightarrow \alpha CO_2 + \frac{\beta}{2}H_2O_{(c)} + \varepsilon_s\,((\lambda-1)O_2 + 3.76\lambda N_2) + \delta SO_2\,. \tag{10}$$

The stoichiometric mole ratio of oxygen to fuel was determined basing on following

$$\varepsilon_s = \frac{n_{O_2(a)}}{n_f} = \left(\alpha + \frac{\beta}{4} - \frac{\gamma}{2} + \delta\right) = \frac{\frac{\dot{n}_{O_2(a)}}{\overline{n}}}{\frac{\dot{n}_f}{\overline{n}}} = \frac{\dot{n}_{O_2(a)}}{\dot{n}_f}\,, \tag{11}$$

where the number of carbon α, hydrogen β, oxygen γ and sulfur δ atoms were identified by the presented system of equations inspired by [20]

$$\begin{cases} \alpha = y_{NG}\sum_{i=1}^{6} y_i\alpha_i + y_{PFO}\sum_{j=1}^{2} y_j\alpha_j \\ \beta = y_{NG}\sum_{i=1}^{6} y_i\beta_i + y_{PFO}\sum_{j=1}^{2} y_j\beta_j \\ \gamma = y_{NG}\sum_{i=1}^{6} y_i\gamma_i + y_{PFO}\sum_{j=1}^{2} y_j\gamma_j \\ \delta = y_{NG}\sum_{i=1}^{6} y_i\delta_i + y_{PFO}\sum_{j=1}^{2} y_j\delta_j \end{cases}. \tag{12}$$

Derived system of equations relates fuels composition (Table 1) with molar fractions of NG and PFO determined by means of relation (6).

The excess air coefficient which is the last of unknown variables of combustion balance (10) has been calculated using assumed molar flow rates of

dry air (Fig. 3), Eqs. (5)–(9) and (11), (12)

$$\lambda = \frac{\varepsilon_a}{\varepsilon_{a(s)}} = \lambda \frac{\varepsilon_{a(s)}}{\varepsilon_{a(s)}} = \lambda \frac{\dfrac{\dot{n}_{a,d(s)}}{\dot{n}_f}}{\dfrac{\dot{n}_{a,d(s)}}{\dot{n}_f}}$$

$$= \frac{\dfrac{\dot{n}_{a,d}}{\dot{n}_f}}{\dfrac{\dot{n}_{a,d(s)}}{\dot{n}_f}} = \frac{\dfrac{\dot{n}_{a,d(s)}}{\dot{n}_f}}{\varepsilon_s \left(1 + \dfrac{\dot{n}_{N_2(a)}}{\dot{n}_{O_2(a)}}\right)} = \frac{\dfrac{\dot{n}_{a,d(s)}}{\dot{n}_f}}{4.762\varepsilon_s}\,. \tag{13}$$

The presented balance substances crossing the considered thermodynamic system boundary (Fig. 2) was obtained by combining the balances (5) and (10)

$$\sum_{i=1}^{m} \dot{n}_i + \sum_{j=1}^{n} \dot{n}_j + \dot{n}_a = \dot{n}_f + \dot{n}_{a,d} + \dot{n}_{\mathrm{H_2O}(a)} = \dot{n}_f \left(1 + \lambda \varepsilon_{a(s)}\right) + \dot{n}_{\mathrm{H_2O}(a)}$$

$$= \dot{n}_f \left[\alpha + (\lambda - 1)\varepsilon_s + 3.762\lambda + \delta + \frac{\beta}{2}\right] + \dot{n}_{\mathrm{H_2O}(a)}$$

$$= \dot{n}_{\mathrm{CO_2}} + \dot{n}_{\mathrm{O_2}} + \dot{n}_{\mathrm{N_2}} + \dot{n}_{\mathrm{SO_2}} + \dot{n}_{\mathrm{H_2O}} = \dot{n}_{ex} = \sum_{k=1}^{5} \dot{n}_k\,. \tag{14}$$

Partial pressures of combustion products components were calculated using Dalton's law

$$p_k = y_k p_{ex} = \frac{\dot{n}_k}{\sum_{k=1}^{n} \dot{n}_k} p_{ex} = \frac{\dot{n}_k}{\dot{n}_{ex}} p_{ex} \tag{15}$$

and molar flow rates balance (14), where the exhaust gas pressure has been assumed as $p_{ex} = p_0$ which implies their mechanical equilibrium with surroundings (the mechanical part of exhaust gas exergy is equal to zero).

2.3 Condensation temperature of H_2SO_4

The sulfuric acid condensation temperature was determined using the Verhoff-Banchero empirical relationship as a following function $T_{\mathrm{H_2SO_4}(c)} = f\left(p_{\mathrm{H_2O}}, p_{\mathrm{H_2SO_4}}\right)$ [21]. Partial pressure of water vapor at equilibrium state $p_{\mathrm{H_2O}}(p_{\mathrm{H_2O}(a)}; p_{\mathrm{H_2O}(\beta)})$ was determined using Eq. (15). It was assumed that water vapor is composed of H_2O molecules introduced with ambient air and H_2O molecules formed in the hydrogen oxidation process. Partial pressure of

sulfuric acid is determined by the efficiency of the oxidation process of sulfur dioxide to sulfur trioxide (assumed $\eta_{SO_3} = 0.05$ [22]) and the efficiency of the gaseous SO_3 and H_2O conversion process to gaseous H_2SO_4 (assumed $\eta_{H_2SO_4} = 1$ [23]). The determined H_2SO_4 condensation temperature was assumed as the minimum temperature of exhaust gas leaving the WHRS.

2.4 The rate of exhaust gas waste heat and exergy

The rate of exhaust gas waste heat and exergy available for recovery was identified on the basis of presented integers using as the integration limits their temperature at the outlet of the turbocharger $T_{ex(1)}$ (Fig. 3) and temperature at the outlet of waste heat recovery process assumed as calculated condensation temperature of sulfuric acid assuming that $T_{ex(2)} = T_{H_2SO_4(c)}$:

$$\dot{Q}_{ex} = \dot{n}_{ex}\Delta\tilde{h}_{ex} = \dot{n}_{ex}\int_{T_{ex(1)}}^{T_{H_2SO_4(c)}} \tilde{c}_p(T)\,\mathrm{d}T, \tag{16}$$

$$\begin{aligned}\dot{B}_{ex} &= \dot{n}_{ex}\Delta\tilde{b}_{ex} = \dot{n}_{ex}\left(\Delta\tilde{h}_{ex} - T_0\Delta\tilde{s}_{ex}\right)\\ &= \dot{n}_{ex}\int_{T_{ex(1)}}^{T_{H_2SO_4(c)}}\left(\tilde{c}_p(T) - T_0\frac{\tilde{c}_p(T)}{T}\right)\mathrm{d}T.\end{aligned} \tag{17}$$

Molar specific heat was calculated using Eq. (15) as the sum of products – mole fractions of combustion products components y_k and their molar specific heats as a function of temperature, $\tilde{c}_{pk} = f(T)$ [24]

$$\tilde{c}_p(T) = \sum_{k=1}^{5} y_k\tilde{c}_{pk}(T) = a_0 + a_1T + a_2T^2 + a_3T^3 = \sum_{n=0}^{3} a_nT^n. \tag{18}$$

Equations (19) and (20) were obtained substituting the polynomial (18) into the Eqs. (16) and (17) and solving the integral within the limits of the identified exhaust gas temperatures

$$\begin{aligned}\Delta\tilde{h}_{ex}\int_{T_{ex(1)}}^{T_{H_2SO_4(c)}}\tilde{c}_p(T)\,\mathrm{d}T &= \sum_{n=0}^{3}\frac{a_n}{n+1}\left(T_{ex(1)} - T_{H_2SO_4(c)}\right)^{n+1}\\ &= \sum_{n=0}^{3}\frac{a_n}{n+1}\Delta T^{n+1},\end{aligned} \tag{19}$$

$$\Delta\tilde{s}_{ex} = \int_{T_{ex(1)}}^{T_{H_2SO_4(c)}} \frac{\tilde{c}_p(T)}{T}\,\mathrm{d}T = a_0 \ln\left(\frac{T_{ex(1)}}{T_{H_2SO_4(c)}}\right) + \sum_{n=1}^{3}\frac{a_n}{n}\Delta T^n. \tag{20}$$

Waste heat quality index ψ which takes into consideration only thermal part of exergy of exhaust gas was determined using following relation

$$\psi = \frac{\dot{B}_{ex}}{\dot{Q}_{ex}} = \frac{\dot{n}_{ex}\Delta\tilde{b}_{ex}}{\dot{n}_{ex}\Delta\tilde{h}_{ex}} = \frac{\Delta\tilde{b}_{ex}}{\Delta\tilde{h}_{ex}} = \frac{\Delta\tilde{h}_{ex} - T_0\Delta\tilde{s}_{ex}}{\Delta\tilde{h}_{ex}} = 1 - T_0\frac{\Delta\tilde{s}_{ex}}{\Delta\tilde{h}_{ex}}. \tag{21}$$

Using the same procedure and assuming that $T_{ex(2)} = T_0$ the available maximum rate of exhaust gas waste heat $\dot{Q}_{ex(0)}$ and exergy $\dot{B}_{ex(0)}$ were determined and used for the comparison with calculated by means of Eqs. (16) and (17) values.

2.5 Evaluation of ideal waste heat recovery process using exhaust gas

Exergy of exhaust gas indicates the maximum theoretical work that can be obtained in the clock-wise reversible thermodynamic cycle realizing ideal energy conversion, i.e. $B_{ex} \equiv W_{ex}$ From this it results that the time rate of exhaust gas exergy flow determines the maximum power that potentially can be generated in the clockwise reversible thermodynamic cycle (maximum time rate of work that can be produced in ideal conditions using exhaust gas as a heat source of reversible cycle, i.e. $\dot{B}_{ex} \equiv \dot{W}_{ex}$. It has been assumed that the rate of effective work transfer through analyzed thermodynamic system boundary (Fig. 2) is delivered to the gearbox which has a common driving shaft with the ideal gas turbine which produces maximum available power in reversible Carnot cycle $\dot{W}_{ex}$ for supporting the ships propulsion system. For the assumed hypothetical system, the presented balance of energy transferred through the thermodynamic system boundary was based on ICE energy balance (1) and calculated by means of Eqs. (16) and (17) the rates of waste heat and exergy of exhaust gas

$$\dot{Q}_f = \dot{Q}_{\mathrm{NG}} + \dot{Q}_{\mathrm{PFO}} = \dot{W}_e + \dot{W}_{ex} + \dot{Q}_{ex(0)} - \dot{Q}_{ex} + \dot{Q}. \tag{22}$$

The presented balance has been rearranged to get the parameter – the energy efficiency gain $\Delta\eta_e\left(\dot{B}_{ex}\right)$ which gives the assesment possibility of

analysed cases

$$1 = \frac{\dot{W}_e + \dot{W}_{ex} + \dot{Q}_{ex(0)} - \dot{Q}_{ex} + \dot{Q}}{\dot{Q}_f} \Rightarrow 1 - \frac{\dot{Q}_{ex(0)} - \dot{Q}_{ex} + \dot{Q}}{\dot{Q}_f} = \frac{\dot{W}_e}{\dot{Q}_f} + \frac{\dot{W}_{ex}}{\dot{Q}_f}$$
$$= \eta_e + \Delta\eta_e \left(\dot{B}_{ex}\right). \tag{23}$$

Using Eqs. (22) and (23) and the maximum rate of exhaust gas exergy $\dot{B}_{ex(0)}$ the maximum energy efficiency gain $\Delta\eta_e \left(\dot{B}_{ex(0)}\right)$ was calculated for the analyzed cases.

3 Analysis results and discussion

The solution to the problems formulated in the introduction was carried out for two sets of operational parameters of a selected engine determined by the set of engine loads $\Gamma = 0.5, 0.85, 1.0$. The lowest load $\Gamma = 0.5$ was chosen based on the highest sulfur mole fraction criterion (Fig. 4), the design load $\Gamma = 0.85$ was chosen based on the highest frequency of occurrence in operational profile. The diagrams in Figs. 4, 5 and 6 were

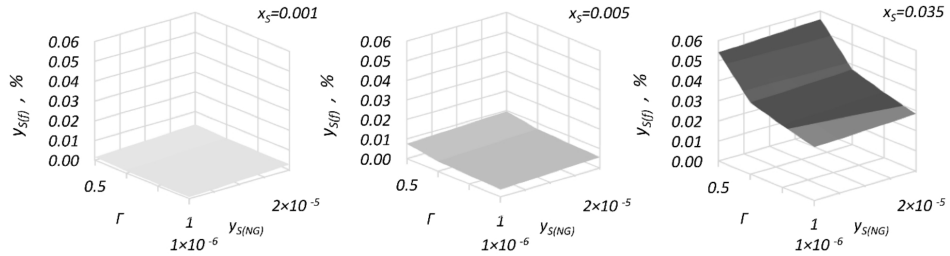

Figure 4: Total sulfur mole fraction in fuel as a function of engine load and sulfur mole fraction in NG.

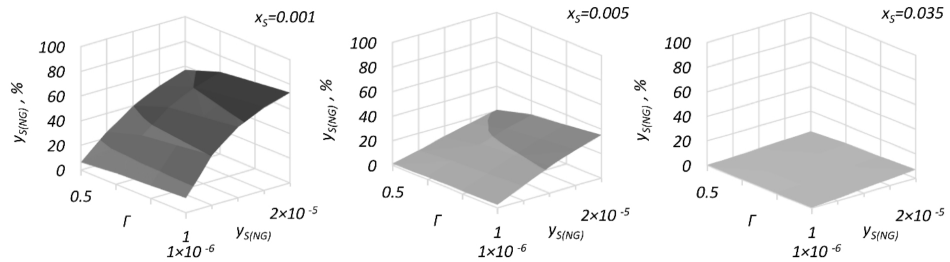

Figure 5: Sulfur mole ratio of NG as a function of engine load and sulfur mole fraction in NG.

calculated for three different values of sulfur mass fraction in PFO, i.e. $x_{S(\mathrm{PFO})} = 0.01, 0.05, 0.035$.

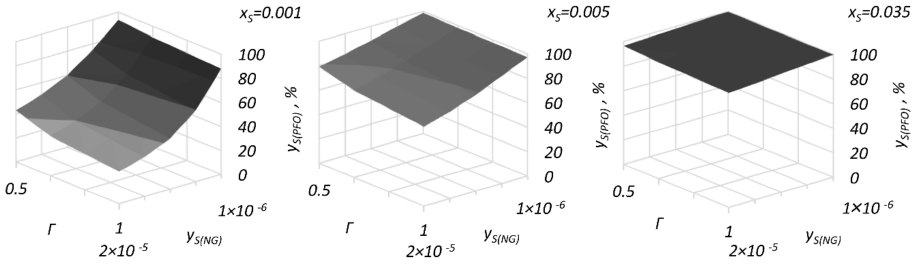

Figure 6: Sulfur mole ratio of PFO as a function of engine load and sulfur mole fraction in NG.

The excess air coefficient and exhaust gas molar flow rate has been calculated in order to determine their composition and basing on components mole fraction their isobaric specific heat as a temperature function (Fig. 7). The same parameters have been calculated for the reference case – when fueling the engine only with FO with 3.5% sulfur mass fraction (Fig. 8).

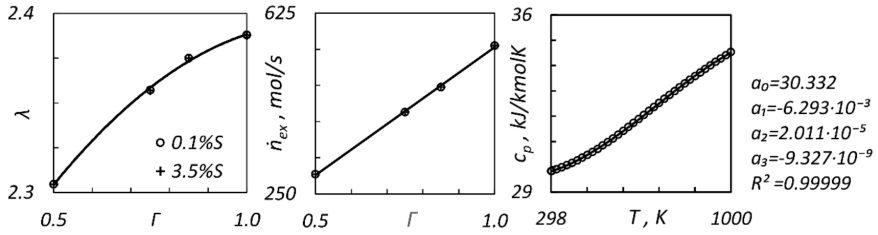

Figure 7: The excess air coefficients, exhaust molar flow rate and isobaric specific heat as a temperature function.

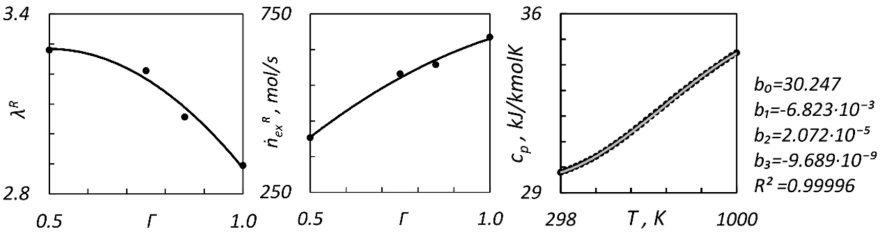

Figure 8: The excess air coefficient, exhaust gas molar flow rate and isobaric specific heat (reference parameters).

The condensation temperature of sulfuric acid and available temperature difference presented in Figs. 9 and 10 has been calculated as a function of sulfur fractions – mole in NG and mass in FO using selected temperatures of exhaust gas as a function of engine load (Fig. 3).

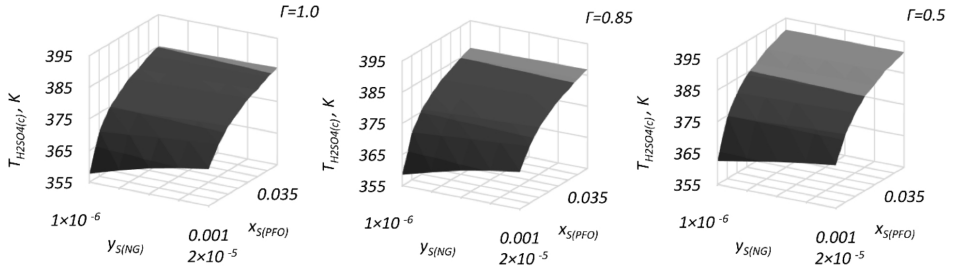

Figure 9: Condensation temperature of sulfuric acid as a function of sulfur fractions – mole in NG and mass in FO.

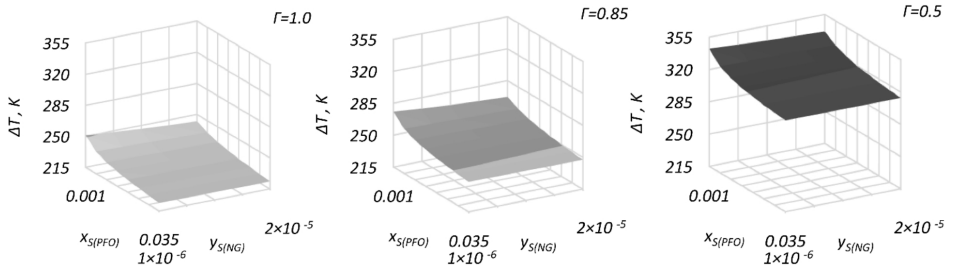

Figure 10: Temperature differences of exhaust gas as a function of sulfur fractions – mole in NG and mass in FO.

Using the calculated rates of exhaust gas waste heat (Fig. 11) and thermal exergy (Fig. 12) the waste heat quality index, presented in Fig. 13, has been determined.

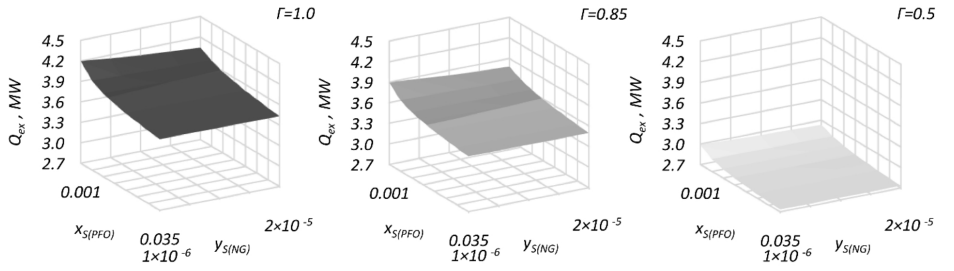

Figure 11: The rate of exhaust gas waste heat as a function of sulfur fractions – mole in NG and mass in PFO.

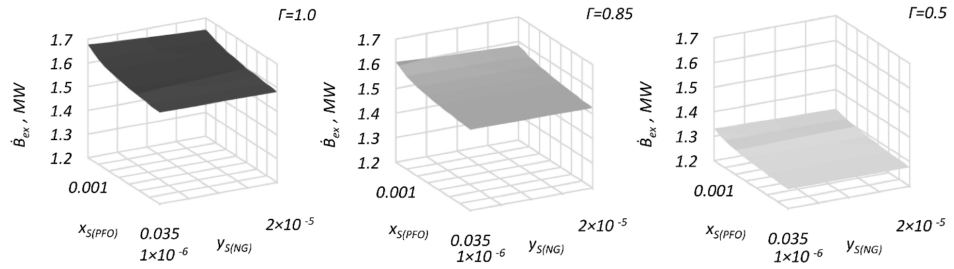

Figure 12: The rate of exhaust gas exergy as a function of sulfur fractions – mole in NG and mass in FO.

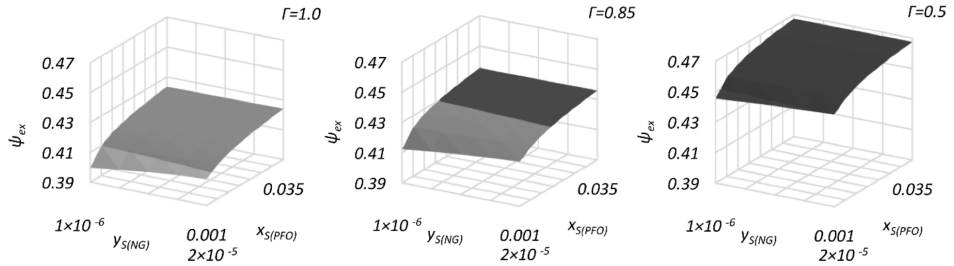

Figure 13: Waste heat quality index of exhaust gas as a function of sulfur fractions – mole in NG and mass in FO.

The same set of parameters as presented has been calculated for two of the reference cases: NG fueling mode with PFO assuming fixed minimum exhaust gas temperature $T_{ex(2)} = 423.15$ K $= idem$ denoted with superscript r (Fig. 14), FO fuelling mode with 3.5% sulfur mass fraction and variable exhaust gas minimum temperature denoted with superscript R (Fig. 15).

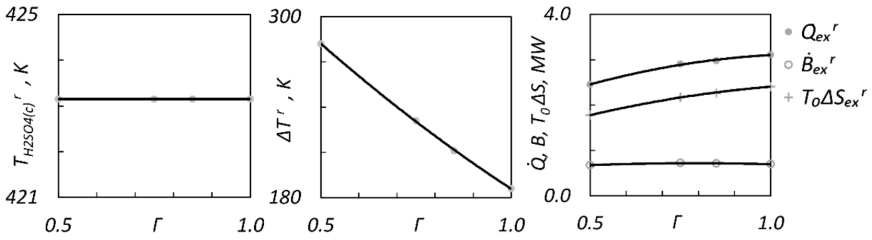

Figure 14: Sulfuric acid condensation temperature, the temperature difference of exhaust gas and the rate of heat and thermal exergy (reference values calculated assuming $T_{ex(2)} = 423.15$ K $= idem$).

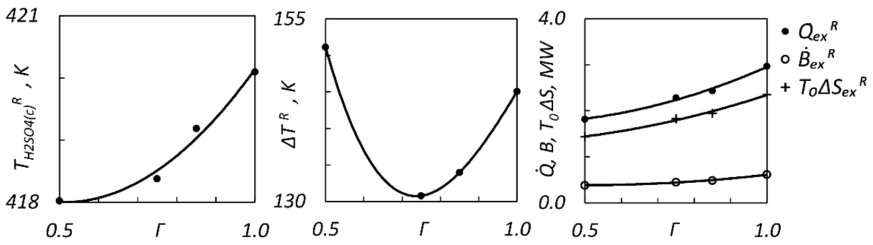

Figure 15: Sulfuric acid condensation temperature, the temperature difference of exhaust gas and the rate of heat and thermal exergy (reference values calculated for FO fueling with 3.5% sulfur mass fraction).

The solved energy balances of selected engine have been presented for NG and PFO fueling in Fig. 16 and for reference case of FO fueling in Fig. 17.

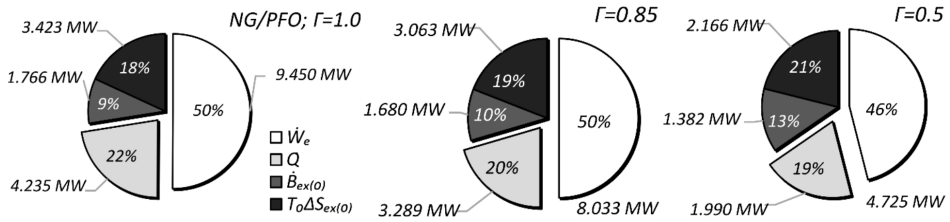

Figure 16: The energy balance of MAN-9L51/60DF when fueling with NG and PFO.

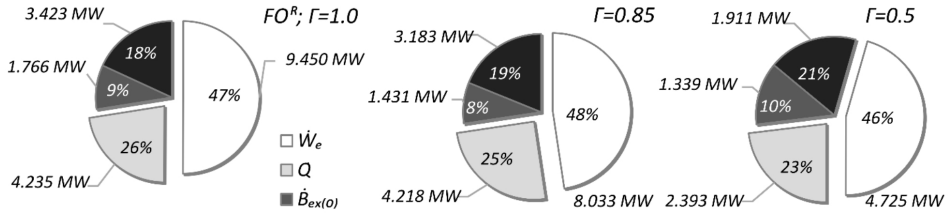

Figure 17: The energy balance of MAN-9L51/60DF when fueling with FO.

The maximum efficiency gain of hypothetical and ideal exhaust gas waste heat conversion system has been shown in Figs. 16 and 17 as a ratio of the rate of exhaust gas exergy when the thermal equilibrium with surroundings is reached and the rate of fuel energy. The efficiency gain under the same assumption of ideal heat recovery but limited by assumption of $T_{ex(2)} = T_{\mathrm{H_2SO_4}(c)}$ has been shown for analysed cases in Fig. 18.

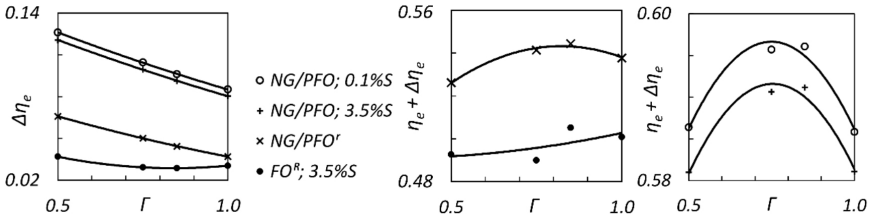

Figure 18: The efficiency gains of exhaust gas heat conversion in ideal Carnot cycle (exergy based).

For the evaluation of all of the analyzed cases the ratios of the rates of recovered exhaust gas waste heat and exergy to their maximum values has been calculated and presented in Fig. 19.

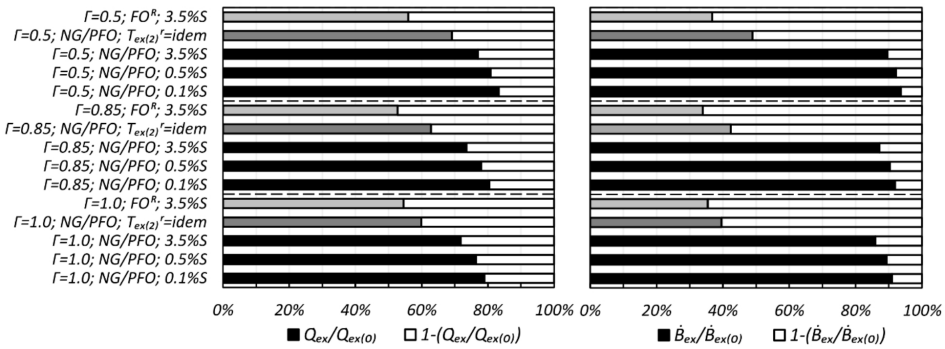

Figure 19: The ratios of exhaust available and maximum waste heat and exergy rates.

According to thermodynamic analysis results the following was observed (notation the same as for identified set of problems):

1. Sulfuric acid condensation temperature is influenced by engine load and sulfur content in fuels (Fig. 4). The significant contribution of NG in total amount of combusted sulfur is observed for maximum analyzed sulfur fractions in gaseous fuel (0.002%) and 0.1% sulfur mass fraction in PFO (Figs. 5 and 6). The highest sulfuric acid condensation temperature occurred at 50% of engine load which corresponded with the highest sulfur fraction in fuels (Fig. 9). Temperature difference of exhaust gas at turbocharger outlet and sulfuric acid condensation presented the same tendency as later (Fig. 10).

2. The highest rate of waste heat and exergy of exhaust gas were observed at 100% load of engine (Figs. 11 and 12) which results from

higher molar flow rate, despite lower exhaust gas temperature differences.

3. More favorable indicators of exhaust gas waste heat quality were observed for the 50% of engine load (Fig. 13). The reason for this is the higher exhaust gas temperatures at lower engine load. An analogous relationship occurs for molar specific exergies. Despite observed differences of analyzed parameters, the thermal exergy flow rates for 100% and 85% engine load are comparable.

4. Fueling of the analyzed engine with NG and PFO with the lowest examined sulfur fractions in both fuels has the highest potential to increase the energy efficiency of analyzed thermodynamic system (Figs. 16, 17, and 18).

5. Similarly to d) fueling of examined engine with NG and PFO achieved the highest rates of available heat and exergy of exhaust gas that can be utilized in ship's WHRS without the risk of low-temperature corrosion occurrence. This waste heat recovery potential is reflected in the highest ratios of available heat and exergy rates and their maximum values, i.e. when thermal equilibrium with surroundings is reached (Fig. 19).

4 Conclusions

The present study has examined the influence of IMO global and local (ECA) regulation of sulfur mass fraction in marine fuels, as well as possible volume fraction of sulfur in NG, on the sulfuric acid condensation temperature of four-stroke DF CI engine's exhaust gas, thus on the rate of its waste heat and exergy. The particular attention has been paid to the possibility of energy efficiency improvement by conversion of waste heat in WHRS into effective power. Above has been assessed only for exhaust gas using exergy to determine effective power generation limits. Thermodynamic analysis has been conducted for the engine load set ($\Gamma = 0.85$) and low load $\Gamma = 0.5,\ 0.85,\ 1.0$.

The results of this study allowed following conclusions to be made:

1. Despite relatively low sulfur volume fractions in NG and mass fraction in pilot FO the condensation of sulfuric acid can occur at high exhaust gas temperatures which are also related with engine load. It indicates

the importance of H_2SO_4 condensation analysis in design process of DF IC engine exhaust gas sensible waste heat recovery systems on ships in order to utilize maximum energy avoiding at the same time low temperature corrosion of heat transfer surfaces.

2. The main limitation of conducted analysis is the idealization of waste energy conversion process whose assumptions cannot be met in real conditions. However, determined boundary values under these assumptions led to another conclusion.

3. The assumption of fixed minimum exhaust gas temperature can lead to significant limitation of the recovered rates of waste heat and exergy, at the same time assuming to low temperature can lead to condensation of sulfuric acid.

The combination of above conclusions and availability of acid-proof engineering materials presented for example in [25] are leading to further research in the field of exhaust gas latent waste heat recovery by introducing condensing heat exchangers to marine power plants.

Received 27 August 2020

References

[1] Lloyd's Register: *Future IMO and ILO Legislation*. 2019.

[2] MAN Diesel & Turbo: *MAN 51/60DF Project Guide*. 2017.

[3] Wu Sh.-Y., Li Ch., Xiao L., Li Y.-R., Liu Ch.: *The role of outlet temperature of flue gas in organic Rankine cycle considering low temperature corrosion*. J. Mech. Sci. .Technol. **12**(2014), 5213–5219.

[4] International Gas Union: *World LNG Report*. 2019.

[5] DNV-GL: *LNG fueled fleet statistics*. http://afi.dnvgl.com/Statistics (accessed 22 Sept. 2019).

[6] Mondejar M.E., Andreasen J.G., Pierobon L., Larsen U., Thern M., Haglind F.: *A review of the use of organic Rankine cycle power systems for maritime applications*. Renew. Sustain. Energ. Rev. **91**(2018), 126–151.

[7] Andreasen J.P., Meroni A., Haglind F.: *A comparison of organic and steam Rankine cycle power systems for waste heat recovery on large ships*. Energies **10**(2017), 547.

[8] Altosole M., Campora U., Laviole M., Zaccone R.: *High efficiency waste heat recovery from dual fuel marine engines*. In: Technology and Science for the Ships of the Future (A. Marinò, V. Bucci, Eds.). Proc. NAV 2018: 19th Int. Conf. on Ship and Maritime Research, Trieste, June 2018. IOS Press, 2018, 21–28.

[9] Singh D.V., Pedersen E.: *A review of waste heat recovery technologies for maritime applications*. Energ. Convers. Manage. **111**(2016), 315–328.

[10] Mikieleiwcz J., Mikielewicz D.: *On the efficient use of a low temperature heat source by the organic Rankine cycle*. Arch. Thermodyn. **34**(2013), 61–73.

[11] Yun E., Park H., Yoon S., Kim K.: *Dual parallel organic Rankine cycle (ORC) system for high efficiency waste heat recovery in marine application*. J. Mech. Sci. Technol. **29**(2015), 2509–2515.

[12] Michos C., Lion S., Vlaskos I., Taccani R.: *Analysis of the backpressure effect of an Organic Rankine Cycle (ORC) evaporator on the combustion products line of a turbocharged heavy duty diesel power generator for marine applications*. Energ. Convers. Manage. **132**(2017), 347–360.

[13] Nawi Z.M., Kamarudin S.K., Sheikh Abdullah R.S., Lam S.S.: *The potential of combustion products waste heat recovery (WHR) from marine diesel engines via organic Rankine cycle*. Energy **166**(2019), 17–31.

[14] Sung T., Kim K.C.: *Thermodynamic analysis of a novel dual-loop organic Rankine cycle for engine waste heat and LNG cold*. Appl. Therm. Eng. **100**(2016), 1031–1041.

[15] Tian Z., Yue Y., Yuan Z., Gu B., Wenzhong G.: *Multi-objective thermo-economic optimization of a combined organic Rankine cycle (ORC) system based on waste heat of dual fuel marine engine and LNG cold energy recovery*. Energies **13**(2020), 1397.

[16] Haglind F., Mondejar M.E., Andreasen J.G., Pierobon L., Meroni A.: *Organic Rankine cycle unit for waste heat recovery on ships (Pilot ORC)*. Danish Technical University, 2017.

[17] CIMAC: *Impact of Gas Quality on Gas Engine Performance*, 2015.

[18] The European Association of Internal Combustion Engine Manufacturers: *Total Sulfur Levels in Natural Gas with Special Consideration of IC Engines*, 2012.

[19] Jeong K., Kessen M.J., Bilirgen H., Levy E.K.: *Analytical modeling of water condensation in condensing heat exchanger*. Int. J. Heat Mass Tran. **53**(2010), 2361–2368.

[20] Szarawara J.: *Chemical thermodynamics*. WNT, Warsaw 1985 (in Polish).

[21] Verhoff F.H., Banchero J.T.: *Predicting dew points of flue gases*. Chem. Eng. Prog. **8**(1974), 71–72,

[22] Cordtz R., Schramm J., Rabe R.: *Investigating SO_3 formation from the combustion of heavy fuel oil in a four-stroke medium-speed test engine*. Energ. Fuel. **10**(2013), 6279–6286.

[23] Maria P.P.: *Condensation of water vapor and acid mixtures from exhaust gases*. Berlin Technical University, 2004.

[24] Burcat A., Ruscic B.: *Third Millennium Ideal Gas and Condensed Phase Thermochemical Database for Combustion with updates from Active Thermochemical Tables*. Argonne National Laboratory, 2005.

[25] Xiong Y., Tan H., Wang Y.W., Mikulčić H., Duić N.: *Pilot-scale study on water and latent heat recovery from flue gas using fluorine plastic heat exchangers*. J. Clean. Prod. **161**(2017), 1416–1422.